Faraday Discussions

Cite this: *Faraday Discuss.*, 2023, **244**, 411

PAPER

View Article Online
View Journal | View Issue

Structural modifications to platinum(II) pincer complexes resulting in changes in their vapochromic and solvatochromic properties†

Mathew J. Bryant,[a] Sara Fuertes,[b] Lauren E. Hatcher,[c] Lynne H. Thomas[a] and Paul R. Raithby *[a]

Received 1st February 2023, Accepted 8th February 2023
DOI: 10.1039/d3fd00025g

There is a need to develop rapidly responsive chemical sensors for the detection of low concentrations of volatile organic solvents (VOCs). Platinum pincer complexes have shown promise as sensors because of their colours and vapochromic and solvatochromic properties, that may be related to the non-covalent interactions between the pincer complexes and the guest VOCs. Here we report an investigation into a series of Pt(II) complexes based on the 1,3-di(pyridine)benzene tridentate (N^C^N) skeleton with the formula [Pt(N^C(R)^N)(CN)] (R = C(O)Me **2**, C(O)OEt **3**, C(O)OPh **4**) with the fourth coordination site occupied by a cyanide ligand. Solid-state samples of the complexes have been tested with a range of volatiles including methanol, ethanol, acetone, dichloromethane and water, and while **2** displays thermochromism, **3** and **4** display rapidly reversible vapochromism and solvatochromism. These results are correlated with X-ray powder and single crystal X-ray structural data including an assessment of the crystal packing and the void space in the crystalline space. The cyanide ligand and the R substituents are involved in hydrogen bonding that creates the voids within the structures and interact with the solvent molecules that influence the Pt···Pt separation in the crystalline state.

Introduction

Square planar platinum(II) complexes are among the classes of small molecules that have shown promise as chemical sensors.[1,2] There are many examples of

[a]*Department of Chemistry, University of Bath, Bath BA2 7AY, UK. E-mail: p.r.raithby@bath.ac.uk*
[b]*Departamento de Quimica Inorgánica, Universidad de Zaragoza, Zaragoza 50009, Spain. E-mail: sfuertes@unizar.es*
[c]*School of Chemistry, Cardiff University, Main Building, Park Place, Cardiff CF10 3AT, UK. E-mail: HatcherL1@cardiff.ac.uk*

† Electronic supplementary information (ESI) available. CCDC 2238847–2238849. For ESI and crystallographic data in CIF or other electronic format see DOI: https://doi.org/10.1039/d3fd00025g

these complexes that show vapochromic or solvatochromic responses to simple analytes in the solid state.[3–9] These colour changes and changes in luminescent properties have been attributed to alterations in intermolecular Pt···Pt contacts and changes in intermolecular non-covalent interactions upon the sorption of volatile organic compounds (VOCs).[3]

Within the general class of square planar platinum(II) complexes the platinum terpyridine pincer complexes [Pt(tpy)X][Y] (where tpy = 2,2′;6′,2″-terpyridine; X = a monodentate anionic ligand; Y = a monoanionic counterion) (Fig. 1(a)) have been extensively studied for their luminescent properties.[10–13] The luminescence observed in these systems, when adjacent molecules pack with Pt···Pt separations of 3.5 Å or less, originates from a low mixed-metal-to-ligand charge-transfer (MMLCT) state, involving an unoccupied π^* state on the terpyridine ligand and a filled $d\sigma^*$ orbital on the Pt centre, primarily derived from the interaction of the d_{z^2} orbitals of adjacent Pt centres.

Several of these luminescent platinum terpyridine pincer complexes or their derivatives display vapochromic or solvatochromic properties. For example, [Pt(Me_2bzimpy)Cl][PF_6] (Me_2bzimpy = 2,6-bis(*N*-methylbenzimidazol-2-yl) pyridine), which crystallises as an orange dimethylformamide (DMF) solvate, turns purple within a matter of seconds when exposed to acetonitrile vapour.[3,4] The related complex [Pt(Me_2bzimpy)Cl]Cl interacts with methanol, ethanol, chloroform and acetonitrile, showing a colour change from orange to red.[3] The solid red complex [Pt(Nttpy)Cl]Cl (Nttpy = 4′-(*p*-nicotinamide-*N*-methylphenyl)-2,2′:6′,2″-terpyridine) changes to an orange colour at room temperature when exposed to methanol.[13]

Also related to the terpyridine systems are the planar cyclometallated pincer complexes, [Pt(N^C^N)X], based on the 1,3-di(2-pyridyl)benzene tridentate (N^C^N) platinum(II) unit (Fig. 1(b)). These complexes are neutral if the fourth ligand position is occupied by a monoanionic ligand (X), and the crystal packing in the solid-state is not moderated by the need for the presence of a counterion, unlike the tpy analogues. Their steric and electronic properties can also easily be modified by the inclusion of substituents on the N^C^N rings. Since the synthesis of the first polyaromatic N^C^N pincer complex [Pt(N^C^N)Cl] in 1999[14] the range of complexes has expanded enormously through the substitution in the *para*-position on the central arene ring,[15–18] or on the two pyridyl rings.[19–22] With these variations it is possible to tune these brightly coloured complexes to exhibit absorptions and emissions spanning the visible spectrum and beyond.[11,23–25] Several of these complexes show colour changes when exposed to solvent vapours

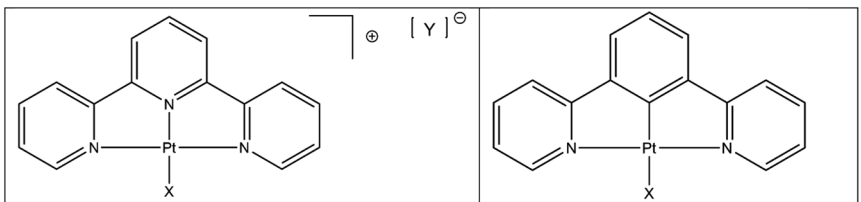

(a) [Pt(tpy)X][Y] (b) [Pt(N^C^N)X]

Fig. 1 Classes of (a) terpyridyl (N^N^N) and (b) cyclometallated (N^C^N) platinum(II) pincer complexes.

or liquids[2,26,27] prompting our investigations into the solvatochromic and vapochromic properties of these materials and their potential use as chemical sensors.

Crystallographic studies of platinum pincer complexes that display either vapochromic or solvatochromic properties indicate that the structures, in the solid-state, contain channels that permit the diffusion of small gaseous or solvent molecules through the crystal lattice. The presence of these molecules and their non-covalent intermolecular interactions with the pincer molecules in the lattice changes the Pt⋯Pt interactions, particularly the extent of the d_{z^2} overlap, and causes the colour change.[28,29]

With these factors in mind we embarked on the synthesis of platinum(II) cyclometallated pincer complexes with a series of different substituents on the *para*-position on the central arene ring and using the anionic cyanide ligand in the fourth coordination site on the Pt(II) centre. The substituents on the central arene ring of the pincer ligand act as spacer groups that alter the separation between adjacent molecules within the crystalline lattice, and thus, potentially, alter the size of the channels within the crystal structure, or at least alter the overall porosity of the crystalline material. The cyanide ligand is an extremely strong-field ligand that is likely to promote luminescence in the complex by displacing the antibonding $d_{x^2-y^2}$ metal orbital, that is known to quench emissive states, to inaccessibly high energies.[23,24] Additionally, in the solid-state the cyanide ligand can act as an effective hydrogen-bond acceptor in interactions with gas or solvent molecules (see Fig. 2).

In our preliminary results we found that the complex [Pt(N^C(R)^N)(CN)] (**1**, R = C(O)OMe) displayed rapidly-reversible absorptive and emissive vapochromic properties with water and methanol.[30] The complex exhibits a yellow anhydrous form that converts reversibly on a subsecond timescale to a red hydrate in the presence of parts-per-thousand quantities of atmospheric water vapour. Similarly, exposure of the anhydrous form to methanol results in a rapid and reversible colour change to a blue methanol solvate. The colour changes are a result of the

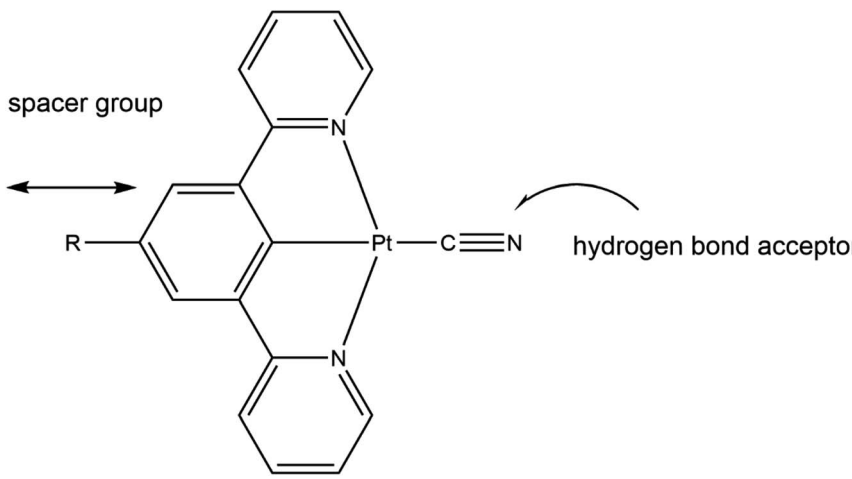

Fig. 2 The role of the substituent R and the cyanide ligand in the [Pt(N^C(R)^N)(CN)] pincer complexes.

water and methanol molecules forming intermolecular hydrogen-bonds with the cyanide ligand of the complex perturbing the Pt···Pt interaction distance in the molecular stacks within the crystal. The presence of the methoxy substituent reduces the crystal packing density and aids the dispersion of the water and methanol molecules through the crystalline solid. The complex can be incorporated as microcrystals into polymer membranes where the vapochromic behaviour remains the same, and the complex has been used to measure the concentration of a gaseous throughflow at the solid–fluid interface.[31]

We now report an extension of this work to investigate the influence of systematically changing the nature of the R group in the [Pt(N^C(R)^N)(CN)] complexes (Fig. 3) on the crystal structure and packing and how these changes alter the vapochromic and solvatochromic response to interactions with a range of volatile solvents and vapours. Through these measurements we hope to identify specific selectivities within the series and establish the rapidity of the colour changes involved to assess whether these complexes might be suitable chemical sensors detecting the presence of volatile solvents.

Experimental

All reactions were carried out under an atmosphere of dry nitrogen using standard Schlenk line techniques. All solvent were dried prior to use using either an automated solvent purification system or through distillation over an appropriate drying agent and stored over molecular sieves. All starting materials were purchased from commercial sources and used without further purification unless otherwise stated. The precursors chloro[acetyl 3,5-di(2-pyridyl)phenyl]platinum, chloro[ethyl 3,5-di(2-pyridyl)benzoato]platinum and chloro[phenyl 3,5-di(2-pyridyl)benzoate]platinum were prepared by modified literature procedures[15]

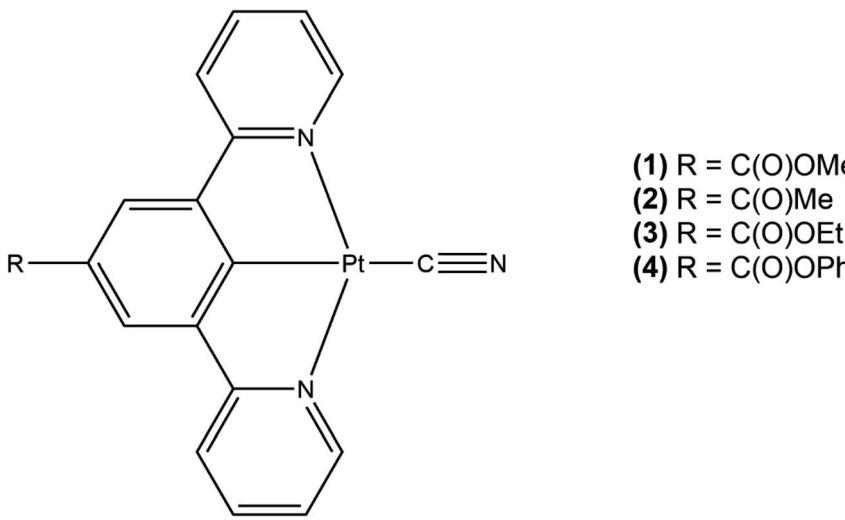

Fig. 3 The series of the platinum(II) pincer complexes to be studied and compared. Complex **1** has already been reported.[30]

and their formulation was confirmed by ^{1}H NMR spectroscopy and mass spectroscopic data (see ESI†).

IR spectra were recorded on a PerkinElmer Spectrum One spectrometer using neat solids. ^{1}H NMR and ^{13}C NMR spectra were recorded on either a Bruker Avance 400 MHz or 500 MHz instrument. Chemical shifts (expressed in parts per million) were referenced to residual solvent peaks. Mass spectra were acquired using a micro TOF electrospray time-of-flight (ESI-TOF) mass spectrometer (Bruker Daltonik GmbH). UV-visible spectra were recorded in the solution state using a PerkinElmer Lambda 650 UV/vis Spectrometer. Thermogravimetric analyses (TGA) were recorded on a PerkinElmer TGA4000 thermogravimetric analyser. Photoluminescence spectroscopy was performed using a PerkinElmer LS55 luminescence spectrometer.

Synthesis

Cyano[acetyl 3,5-di(2-pyridyl)phenyl]platinum (2). To a stirred suspension of freshly prepared AgCN (26.6 mg, 0.199 mmol) in 30 ml of acetonitrile and dichloromethane (1 : 1), chloro[acetyl 3,5-di(2-pyridyl)phenyl]platinum (100 mg, 0.199 mmol) was added, and heated under reflux for 24 h at 85 °C under a nitrogen atmosphere. The resulting suspension was dried under reduced pressure, and then stirred with dichloromethane (30 ml) until the residues were dissolved. The pale-yellow mixture was then filtered, and solvents removed *in vacuo*. The resulting green solid, was washed with an excess of diethyl ether resulting in pure product. Yield: 30 mg, 30.6%.^{1}H NMR (400 MHz, $CDCl_3$) δ_H: 8.90 (d, $^{3}J_{H-H} = 5.0$ Hz, $^{3}J_{H-Pt} = 46.3$ Hz, 2H, *ortho*-Py), 7.95 (t, $^{3}J_{H-H} = 8.0$ Hz, 2H, *para*-Py), 7.88 (s, 2H, pincer-Ph), 7.71 (d, $^{3}J_{H-H} = 7.7$ Hz, 2H, *meta*-Py), 7.19 (t, $^{3}J_{H-H} = 6.0$ Hz, 2H, *meta*-Py), 2.56 (s, 3H, $COCH_3$). ^{13}C[24,30] NMR (101 MHz, $CDCl_3$) δ_C: 201.5, 171.0, 159.0, 146.9, 143.4, 137.4, 128.4, 127.5, 123.9, 30.1. Low solubility did not allow detection of all quaternary carbons. IR (cm^{-1}): ν(C≡N) 2114, ν(C=O) 1677. Mass spectrometry (positive loop injection): measured (MeOH) *m*/*z* – 517.0678, calculated for $[C_{19}O_1N_3H_{13}Pt][Na]^+$ – 517.0678 – correct isotope pattern.

Cyano[ethyl 3,5-di(2-pyridyl)benzoato]platinum (3). To a stirred suspension of freshly prepared AgCN (26.6 mg, 0.199 mmol) in 30 ml of acetonitrile and dichloromethane (1 : 1), chloro[ethyl 3,5-di(2-pyridyl)benzoato]platinum (106 mg, 0.199 mmol) was added, and heated under reflux for 24 h at 85 °C under a nitrogen atmosphere. The resulting suspension was dried under reduced pressure, and then stirred with dichloromethane (30 ml) until the residues were dissolved. The pale-yellow mixture was then filtered, and solvents removed *in vacuo*. The resulting yellow/orange solid, was washed with an excess of diethyl ether resulting in pure product. Yield: 30 mg, 30.6%. ^{1}H NMR (500 MHz, $CDCl_3$) δ_H: 9.28 (d, $^{3}J_{H-H} = 5.8$ Hz, $^{3}J_{H-Pt} = 47.3$ Hz, 2H, *ortho*-Py), 8.20 (s, 2H, pincer-Ph), 8.05 (t, $^{3}J_{H-H} = 7.8$ Hz, 2H, *para*-Py), 7.84 (d, $^{3}J_{H-H} = 7.8$ Hz, 2H, *meta*-Py), 4.46 (q, $^{3}J_{H-H} = 7.1$ Hz, 2H, CO_2CH_2), 1.48 (t, $^{3}J_{H-H} = 7.1$ Hz, 3H, $CO_2CH_2CH_3$). ^{13}C[30] NMR (101 MHz, $CDCl_3$) δ_C: 179.9, 167.7, 166.6, 155.7, 153.5, 143.2, 139.6, 136.9, 126.7, 125.0, 124.6, 120.3, 61.3, 14.5. IR (cm^{-1}): ν(C≡N) 2111, ν(C=O) 1702. Mass spectrometry (positive loop injection): measured (MeOH) *m*/*z* – 547.0688, calculated for $[C_{20}O_2N_3H_{15}Pt_1][Na]^+$ – 547.070599. Correct isotope pattern.

Cyano[phenyl 3,5-di(2-pyridyl)benzoato]platinum (4). To a stirred suspension of freshly prepared AgCN (26.6 mg, 0.199 mmol) in 30 ml of acetonitrile and

dichloromethane (1 : 1), chloro[phenyl 3,5-di(2-pyridyl)benzoato]platinum (115 mg, 0.199 mmol) was added, and heated under reflux for 24 h at 85 °C under a nitrogen atmosphere. The resulting suspension was dried under reduced pressure, and then stirred with dichloromethane (30 ml) until the residues were dissolved. The pale-yellow mixture was then filtered, and solvents removed *in vacuo*. The resulting purple solid, was washed with an excess of diethyl ether resulting in pure product. Yield: 30 mg, 30.6%. ^{1}H NMR (400 MHz, $CDCl_3$) δ_H: 9.32 (d, $^{3}J_{H-H} = 5.3$ Hz, $^{3}J_{H-Pt} = 46.1$ Hz, 2H, *ortho*-Py), 8.36 (s, 2H, pincer-Ph), 8.10 (td, $^{3}J_{H-H} = 7.7$ Hz, $^{4}J_{H-H} = 1.5$ Hz, 2H, *para*-Py), 7.90 (d, $^{3}J_{H-H} = 7.7$ Hz, 2H, *meta*-Py), 7.53 (t, $^{3}J_{H-H} = 7.6$ Hz, 2H, *meta*-ester-Ph), 7.37 (t, $^{3}J_{H-H} = 7.3$ Hz, 4H, *meta*-Py + *para*-ester-Ph), (*ortho*-ester-Ph obscured by $CDCl_3$). ^{13}C {^{1}H} NMR (125 MHz, $CDCl_3$) δ_C: 180.4, 167.4, 165.4, 155.6, 150.8, 147.4, 143.5, 139.8, 136.1, 129.6, 126.1, 125.5, 124.9, 121.6, 120.4. Low solubility did not allow detection of all quaternary carbons. IR (cm^{-1}): ν(C≡N) 2116, ν(C=O) 1725. Mass spectrometry (positive loop injection): measured (MeOH) m/z – 595.0787, calculated for $[C_{24}O_2N_3H_{15}Pt_1][Na]^+$ – 595.070634 – correct isotope pattern.

X-ray crystallography

Single crystal X-ray diffraction. Suitable single crystals were mounted on glass fibres with perfluoroether oil and transferred to a diffractometer. Single crystal X-ray diffraction data was collected on an Oxford Diffraction Gemini A Ultra diffractometer equipped with a Cryojet XL, and using monochromated Mo-K_α radiation or on an Agilent Technologies SuperNova diffractometer equipped with a 700 Series Oxford Cryosystems Cryostream and using monochromated Cu-K_α radiation. The crystal data, data collection parameters, and structure solution and refinement details are summarised in the ESI (Tables S1–S22†). The structures were solved using SIR-2002 [32] and refined by full-matrix least-squares based on F^2 using SHELXL-2014 [33] in the OLEX2 suite.[34] All non-hydrogen atoms were refined with anisotropic displacement parameters and hydrogen atoms were placed in idealised positions and allowed to ride on the relevant carbon atoms. Isotropic displacement parameters for the hydrogen atoms were set at 1.2 U_{eq} of the aromatic carbon atoms and 1.5 U_{eq} for the methyl hydrogen atoms; the methyl groups were refined as rigid bodies. The hydrogen atoms on the solvent water molecules were not located and were not included in the refinement cycles. In structure **2′** an attempt was made to model the disordered solvent in the channels (probably water and acetone) by assigning the largest peaks as water molecules and assigning them isotropic displacement parameters. Refinements were continued until convergence was reached and the residual electron density maps showed no chemically sensible residual features.

Powder diffraction. Powder diffraction experiments were performed using 0.5 mm capillaries, on an Oxford Diffraction Gemini A Ultra diffractometer, using graphite monochromated Mo-K_α radiation, equipped with a CryojetXL cooling device. Simulated powder patterns from single crystal data were generated using Powdercell.[35]

Results and discussion

The platinum(II) pincer complexes **2**, **3** and **4** were prepared following the same general synthetic methodology as previously reported for complex **1** (Fig. 3).[30] The

complexes were characterised by IR and ^{1}H and ^{13}C NMR spectroscopies and by mass spectrometry. In the IR spectra of the three complexes each showed stretching frequencies characteristic of the cyanide and carbonyl groups around 2114 cm^{-1} and 1700 cm^{-1}, respectively. The TOF electrospray time-of-flight (ESI-TOF) mass spectra showed ions corresponding to the $[Na]^{+}$ salt and the correct isotope patterns for the chemical formula.

The study of complex **1** had shown that the vapochromic and solvatochromic behaviour in the solid state was associated with the intermolecular interactions between the pincer complex and the water or methanol molecules and also the Pt⋯Pt stacking interactions. It was appropriate to determine the crystal structures of the new complexes in the presence or absence of solvent molecules and establish whether Pt⋯Pt stacking occurred in the anhydrous and solvated forms, if possible, correlating the structural data with the vapochromic or solvatochromic behaviour. In **1** in the red form, [Pt(N^C(C(O)OMe)^N)(CN)]·H_2O, there is an extended hydrogen-bonding network that bridges between the cyanide ligands on adjacent pincer complexes, and brings the Pt-centres close enough to interact at a distance of 3.452(3) Å. This degree of metal⋯metal interaction facilitates triplet metal–metal-to-ligand charge-transfer (^{3}MMLCT), also observed in related platinum complexes.[36,37] In the yellow anhydrous form of **1**, [Pt(N^C(C(O)OMe)^N)(CN)], there is no solvent mediated hydrogen-bonding network, and in the crystal structure there is a staggered arrangement of pincer molecules with an increase in Pt⋯Pt separation to 3.663(1) Å. While in the blue methanol solvated form of **1**, [Pt(N^C(C(O)OMe)^N)(CN)]·MeOH, the methanol molecules participate in a hydrogen-bonding, with each methanol molecule hydrogen bonding to one cyanide group on a nearby pincer molecule. This facilitates a shorter Pt⋯Pt stacking interaction with the shortest Pt⋯Pt distance of the three at 3.388(1) Å. These small changes in the Pt⋯Pt interaction distance and the metal⋯metal orbital overlap influence the ^{3}MMLCT transitions in each of the three forms and thus provide an explanation for the vapochromic response. This combination of vapochromic and structural data provides a benchmark for the studies described for complexes **2**, **3** and **4**, described here.

Cyano[acetyl 3,5-di(2-pyridyl)phenyl]platinum 2

Vapochromic and solvatochromic properties of 2. In complex **2** the substituent ester group of **1** has been replaced by the smaller acetyl group, and there is only one hydrogen bond acceptor oxygen compared to two in **1**. Complex **2** was tested for its vapochromic and solvatochromic properties with a range of volatile organic solvents. However, the observed behaviour of **2** is somewhat different to that reported for **1**. In the solid-state the complex **2** exists in a green form (form-I), and appears unaffected by the flow of dry gas or the application of solvents. However, upon strong heating (transition beginning at *ca.* 140 °C) the compound does display thermochromism, from green to yellow (form-II) (Fig. 4). This is irreversible, however, and the compound remains yellow under ambient conditions, unless re-dissolved and precipitated. This colour change was hypothesised to be the loss of solvated water from the green form as the driving force for the transition, as seen with the red and yellow forms of **1**.

In order to confirm whether or not the colour change involves the loss of water, IR spectra were run on the solid-state before and after the transformation. These

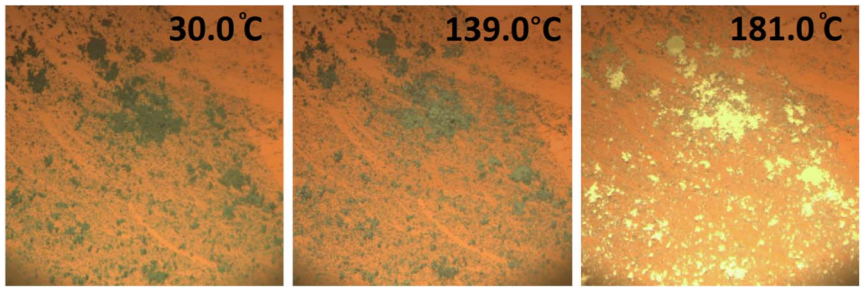

Fig. 4 Hot-stage microscope images of **2** displaying the colour transformation.

could be recorded straightforwardly because of the irreversibility of the transition. The spectra are largely identical (Fig. S1†), however upon transformation to form-II, there is the complete loss of a broad signal at 3405 cm^{-1}. This broad signal is highly characteristic of water as part of a hydrogen bonding network.[38] The only other differences between the two spectra can be seen as small shifts in the peaks assigned to the $\nu_{C\equiv N}$ and $\nu_{C=O}$: to 2108 cm^{-1} and 1670 cm^{-1}, respectively. These small changes are consistent with changes in the hydrogen bonding associated with the loss of water. The loss of water from the green form of **2** was further confirmed by a thermogravimetric analysis. The result indicates that there is a two-step loss of 3.45% which corresponds to 17.67 g mol^{-1} or one equivalent of water (Fig. S2†).

Powder X-ray diffraction has been used to assess whether the green to yellow transition was a result of a structural transition. First, a powder pattern was recorded for a sample of the green powder in an open-ended capillary. This was then heated until the sample had visibly changed completely to yellow, and the diffraction pattern remeasured. The patterns produced are of low resolution (measured using an in-house diffractometer), but they serve well as a finger-printing tool, and it is at first immediately clear that both the forms are crystalline, giving defined diffraction patterns. It is also apparent that the crystal structure has transformed as a result of heating, producing a markedly different pattern (Fig. S3†), indicating that a very definite structural transition coincides with the colour change, as observed for **1**.

A further powder diffraction experiment was performed to track the structural changes between the forms, a second capillary of the green powder was prepared (with one open end for water to leave), and the temperature scanned between 300–390 K measuring the diffraction pattern at 10 K intervals. The experiment (Fig. S4†) resulted in a phasing-out of the green form-I pattern with simultaneous phasing-in of the yellow form-II pattern, as the temperature increases. This suggests a definite and rapid crystalline switch, with no detectable intermediates.

Single crystal X-ray structure of the green form of 2 (form-I). In order to complete the analysis of the structural nature of the thermochromic process observed for **2**, single crystal X-ray structural analyses were attempted on crystals of the green and yellow forms. Unfortunately, obtaining crystals of the green form suitable for an X-ray experiment proved impossible, but it was possible to obtain single crystals of the yellow form.

During the crystallisation experiments, it was possible to obtain alternative green crystals from the solvent mixture that do not display the same diffraction pattern with that of the bulk powder but may be a different solvate of the thermochromic green material with a different solvent mixture. The structure of these crystals was determined, admittedly to a low quality, partly attributed to the quantity of disordered solvent present in the crystal. While this structure does not accurately represent the structure of the bulk thermochromic powder, it does offer us some insights into the possible structure of the powder. The similar colouration for example suggests there may be a comparable level of intermolecular interaction between the platinum centres.

The crystal of the green form of **2** (designated **2′** to differentiate it from the structure of the bulk form) was obtained by vapour diffusion of *n*-hexane into a water/acetonitrile solution. **2′** crystallised in the orthorhombic space group *Ibam*, with the asymmetric unit consisting of half a neutral molecule of **2′**, one defined molecule of water, and a large quantity of disordered solvent (Fig. 5). The complex lies on a crystallographic mirror plane so that the whole structure is planar with the C(O)Me substituent required to be in the same plane as the three six-membered rings, the Pt atom and the cyanide group. The complex adopts the expected square planar coordination geometry at the Pt(II) centre, with the cyanide group being situated *trans* to the coordinated aryl ring. The angles at the Pt(II) display minor distortions from the idealized geometry (N1–Pt1–N2 159.4 (10)°) because of the pincer bite angle, with bond parameters in the expected ranges (Table 1).[39–41]

The extended structure of the crystal consists of layers of planar units of **2′** arranged into columns, with significant levels of platinum–platinum interaction (Pt–Pt–Pt angle of 177.20 (6)°). The molecules also alternate between two planar orientations, separated by a torsion of 47.93° (taken as angle between planes [C19, Pt1, C19$^{\#}$, Pt1$^{\#}$] and [C19$^{\$}$, Pt1$^{\$}$, C19$^{\&}$, Pt1$^{\&}$] where $\# = (x, y, 1 + z)$, $\$ = (x, \frac{1}{2} - y, \frac{1}{2} + z)$, $\& = (x, \frac{1}{2} - y, -\frac{1}{2} + z)$) (Fig. 6). The Pt⋯Pt interaction distance along these stacks is 3.319(1) Å which is slightly shorter than the Pt⋯Pt distances of 3.452(3) Å and

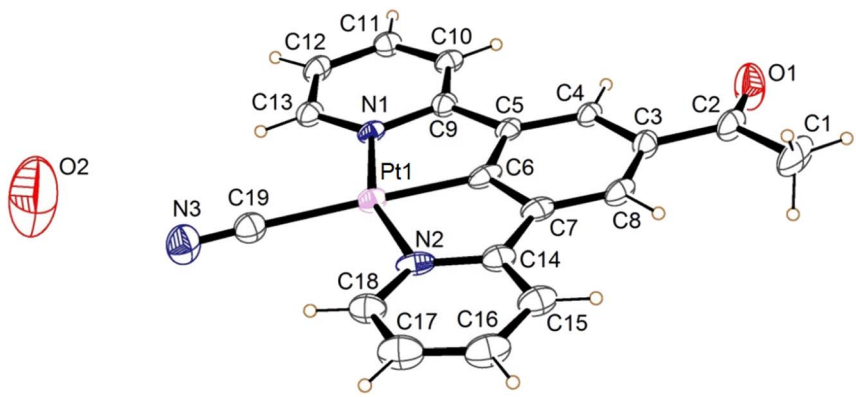

Fig. 5 The asymmetric unit of **2′** (green form) as determined by single crystal X-ray diffraction. The crystal was not of sufficient quality to resolve the water hydrogen atoms. Disordered solvent molecules have been omitted for clarity. Displacement ellipsoids are set at 50% probability.

Table 1 Bond lengths at the Pt(II) centre in 2′ (green)

Bond	Length (Å)
Pt1–N1	2.024(18)
Pt1–N2	2.083(22)
Pt1–C6	1.946(28)
Pt1–C19	2.033(31)
C19–N3	1.182(38)

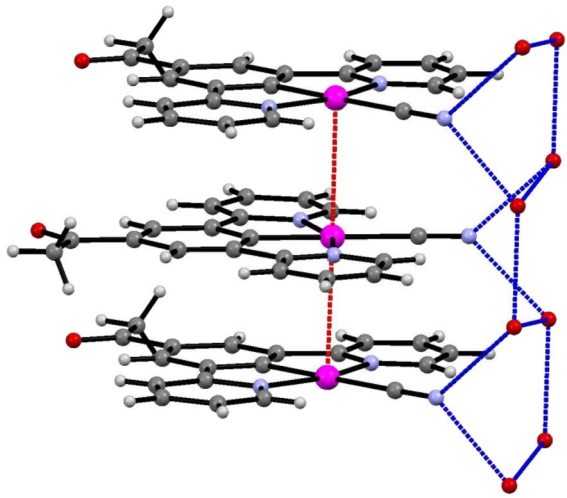

Fig. 6 The stacks of 2′, highlighting the platinum–platinum interactions (red) and hydrogen bonding of the water to the cyanide groups (blue).

Table 2 Hydrogen bond distances involving the solvent water molecule in 2′ (green)

H-bond[a]	Distance (D···A) (Å)
O2···N3	2.68 (6)
O2···O2′	3.26 (6)
O2···O2″	2.61 (5)

[a] $' = (x, 1 - y, \frac{1}{2} + z)$, $'' = (x, y, 2 - z)$.

3.388(1) Å in the red and blue forms of **1**, respectively. Each molecule of 2′ is hydrogen bonded to the structurally ordered water molecule *via* the cyanide ligand, which are then arranged into a network of water that extends along the *c*-axis (Table 2).

The crystal structure is porous, with a large void that runs along the *c*-axis. By omitting the occupying solvent molecules, the channels take up 35.6% of the total crystal volume. The channel contains disordered solvent that it was not possible to resolve crystallographically, although an attempt was made to model some of

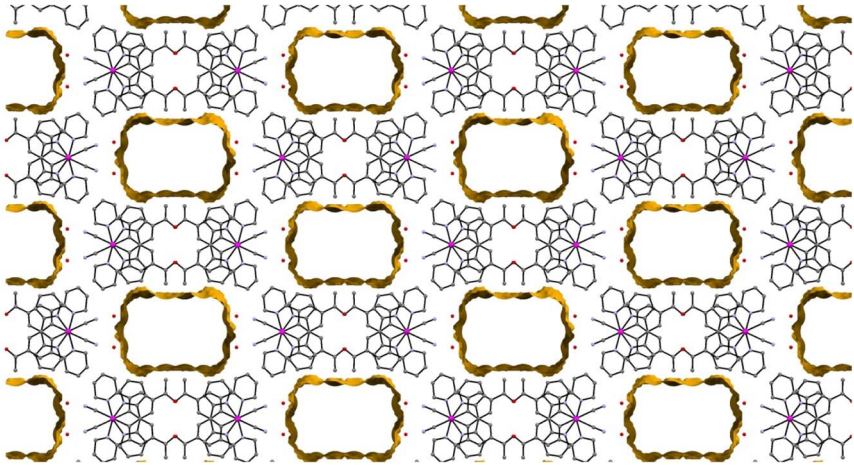

Fig. 7 The view along the *c*-axis of 2′ with the large pores highlighted. The disordered solvent within these pores is not shown.

the largest residual peaks by assigning them as water molecules. It is that the channels contain a mixture of water and acetonitrile (Fig. 7). The formation of such a large pore is unusual in this class of complexes. As can be seen in Fig. 6 the stacks of molecules along the *c*-axis are similar to those observed in **1** with planar molecules, in two alternating orientations and Pt⋯Pt interactions.[30] It is interesting to understand how a minor change in structure between **1** and 2′, replacing an ester group by a smaller acetyl substituent, has such a major influence on the crystal packing, generating large pores through the structure, resulting in different solvatochromic properties. In the crystal structure of 2′ the weak C–H donor hydrogen bonding interactions play a different role to those in **1** forming

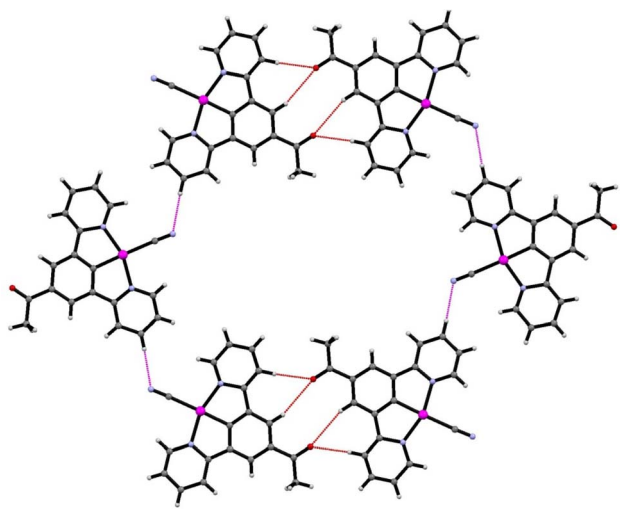

Fig. 8 Details of the weak hydrogen bonding interactions in the crystal structure of 2′.

Table 3 C–H hydrogen bonding interactions involved in the channel formation in **2′** (green)

Bond[a]	Distance (D···A) (Å)	Distance (H···A) (Å)	Angle (D···H···A) (°)
C10–H10–O1*	3.274 (21)	2.345	176.06
C4–H4–O1*	3.685 (21)	2.786	162.91
C16–H16–N3^{+}	3.352 (23)	2.422	121.76

[a] * = $(1-x, 1-y, z)$, + = $(\frac{1}{2}-x, -\frac{1}{2}+y, 1-z)$.

rings between the pincer molecules in the same layer of the crystal (Fig. 8). Unlike in **1** there are no interactions between the cyanide and the substituent group (acetyl) in **2′** and the orientation is completely different such that that interaction to this group bridged by solvent is impossible. It appears that the replacement of the ester with an acetyl group has prevented this type of inter-stack interaction. In the absence of this interaction, there are in-plane weak hydrogen bonding interactions from the pincer to the cyanide and carbonyl groups, which in turn leads to the formation of a large ring of molecules. These rings then stack *via* Pt···Pt interactions to create the pores of the structure. Details of these hydrogen bonding interactions are listed in Table 3.

Single crystal structure of the yellow form of 2 (form-II). The crystal structure of the yellow form of **2** (form-II), obtained after heating, was also determined. Yellow single crystals were obtained by evaporative crystallisation from a dry acetonitrile solution. The compound crystallised in the monoclinic space group $P2_1/c$. This form contains one neutral molecule of **2** in the asymmetric unit (Fig. 9). The molecular structure of the molecule is very similar to that of the green form (form-I), and again, the platinum centre adopts the expected square planar geometry, with minor distortion (N1–Pt1–N2 angle 159.90 (10)°) because of the pincer bite angle, with bond parameters in the expected ranges (Table 4).[39–41] There is good agreement between the X-ray powder pattern obtained for the

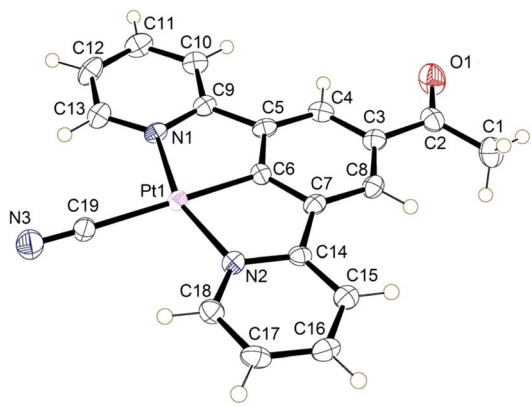

Fig. 9 The molecular structure of the yellow form of **2** (form-II). Displacement ellipsoids are set at 50% probability.

Table 4 Bond lengths around the Pt(II) centre in **2** (yellow)

Bond	Length (Å)
Pt1–N1	2.034(3)
Pt1–N2	2.043(3)
Pt1–C6	1.934(3)
Pt1–C19	2.058(3)
C19–N3	1.148(5)

yellow, bulk crystalline sample of **2** obtained after heating and the simulated powder pattern calculated from the crystal structure determined for the yellow form of **2** (form-II) (Fig. S5†) and it is apparent that the minor change to the pincer group has greatly altered the way the compound packs in the absence of water.

The crystal packing in the structure of the yellow complex **2** (Fig. 10 and 11) consists of stacks of end-to end pairs of pincer molecules, themselves arranged into a herringbone orientation (two orientations of stacks) so that there are essentially no longer planar layers in the crystal with Pt⋯Pt stacks perpendicular to them. Platinum–platinum separations within the pairs are 4.813 (1) Å and 5.341 (2) Å which indicates that there are no direct metal⋯metal interactions in the structure as is the case in the yellow form of **1**. Weak C–H donor hydrogen bonding interactions are present both within each pair, between pairs in the stacks, and between the stacks, which involve either the cyanide or carboxylate groups. Details of these interactions can be found in Table 5.

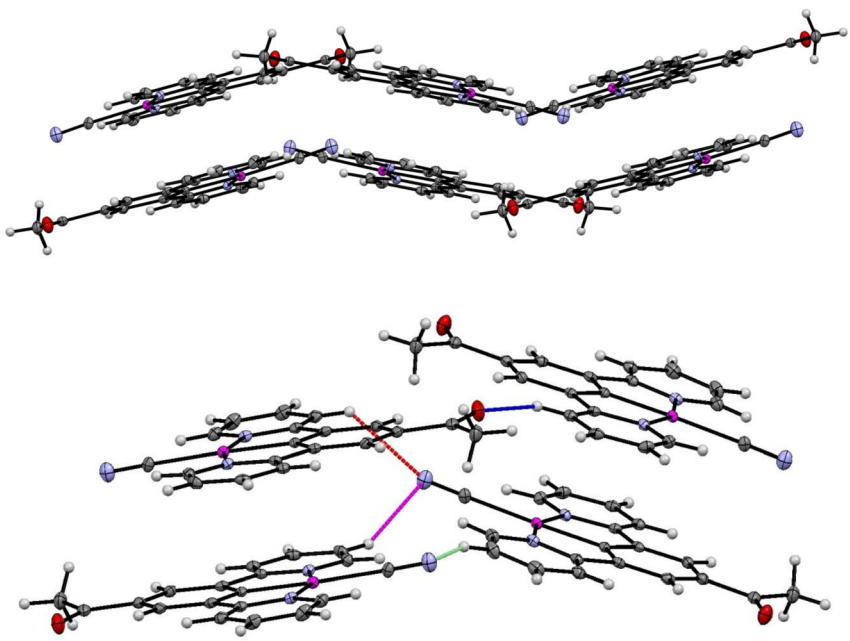

Fig. 10 (Top) Herringbone arrangement in the yellow form of **2**. (Bottom) Weak hydrogen bonding interactions between the two orientations of the herringbone structure.

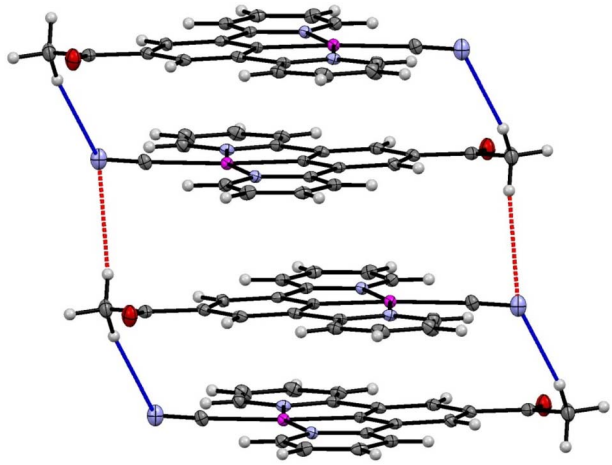

Fig. 11 Weak hydrogen bonding interactions within and between pairs of molecules of the yellow form of **2** (form-II).

Table 5 C–H donor hydrogen bond interactions in the yellow form of **2** (form-II)[a]

Bond[a]	Distance (D···A) (Å)	Distance (H···A) (Å)	Angle (D···H···A) (°)
C1–H1C–N3^{1}	3.736 (6)	2.891	147.42
C1–H1B–N3^{2}	3.742 (6)	2.792	170.35
C12–H12–N3^{3}	3.315 (5)	2.526	142.80
C15–H15–O1^{4}	3.148 (5)	2.447	132.20
C17–H17–N3^{5}	3.721 (5)	2.867	153.29
C10–H10–N3^{6}	3.460 (5)	2.788	130.08

[a] $1 = (-x, -y, 1-z)$, $2 = (1-x, -y, 1-z)$, $3 = (x, \frac{1}{2}-y, \frac{1}{2}+z)$, $4 = (x, -\frac{1}{2}-y, -\frac{1}{2}+z)$ $5 = (x, \frac{1}{2}-y, -\frac{1}{2}+z)$, $6 = (1-x, -\frac{1}{2}+y, 1.5-z)$.

It is clear from the extended structure (Fig. 10) that there are significant differences in arrangement from those observed in the crystal packing of **1**, and from the packing in the green form of **2′** (form-I). As with the green crystal, there is no interaction between the acetyl group and adjacent cyanides, but it is also non-planar. The absence of this interaction between the cyanide and the substituted group of the pincer could be the important difference that prevents reversible transitions between hydrates/solvates and the anhydrous form for this complex, when compared to **1**. It may be the case looking at **1** that the interaction between the ester and adjacent cyanides stabilises the solvent-free structure in a planar configuration that allows for re-insertion of water or other solvents, leading to the observed vapochromic and solvatochromic properties.

Although for **2** the structure of the thermochromic green form has not been determined, however, based on other experimental data and the nature of the alternative green form produced **2′**, it may be hypothesised that they share similarities. It is likely that the green form-I is a planar, platinum stacked

structure, as evidenced by the green coloration. It has also been shown that water is present in the structure.

Based on this, it may be proposed that due to a lack of the weak intermolecular interactions to adjacent cyanides, provided by the ester group, planar structures facilitating platinum–platinum interactions for complex **2** are only stable in the presence of water. The transition to a buckled herringbone yellow form, unable to re-accept water occurs once water is evacuated, and it may follow that the dissimilarity of this structure to any seen for this class of complexes so far (*i.e.* lack of planarity) may be the cause for this lack of reversibility.

Cyano[ethyl 3,5-di(2-pyridyl)benzoato]platinum (3)

Synthesis and characterisation of complex 3. From the previous results obtained for **2** a possible hypothesis is that the intermolecular interactions provided by an ester are necessary in stabilising the crystal structure to the extent where solvents can exit but also for the basic structure to remain in a configuration where they may re-enter the structure. Therefore, a study of pincer complexes with larger ester substituents was undertaken.

An ethyl analogue of the pincer ester was synthesised by esterifying 1,3-dibromobenzoic acid, and then performing Stille-coupling,[42] then performing cyclometallation[15] and salt metathesis steps as with **1** to obtain **3**.

Complex **3** was fully characterised by NMR and IR spectroscopy, mass spectrometry and X-ray crystallography. The ethyl signal was clearly visible in the ^{1}H NMR spectrum. The IR spectrum shows a strong, sharp absorption at 2111 cm^{-1} assignable to the $\nu_{C\equiv N}$ of a cyanide group. This value is consistent with those recorded for a series of related compounds.[43,44] Also seen is a single strong absorption at 1702 cm^{-1} assignable to the $\nu_{C=O}$ of the ester group, which is a typical value for an ethyl benzoate ester.

Vapochromic and solvatochromic behaviour of complex 3. Like **1**, complex **3** displays colour changes through interaction with solvent vapour. However, the interactions are significantly different. The compound when precipitated from methanol under atmospheric conditions appears yellow/orange in colour. Upon application of solvent vapour (methanol, ethanol or dichloromethane) an extremely rapid transformation to a stable green form occurs (Fig. 12). The complex can be transitioned equally rapidly back to the orange form, through direct application of water. Unlike **1** atmospheric water vapour is insufficient to

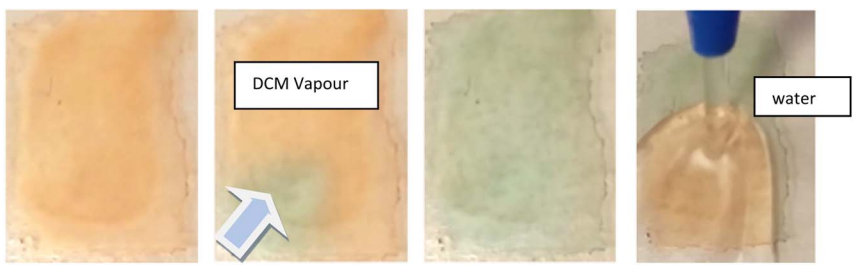

Fig. 12 Photographs showing the solvent interactions of **3**. (Left) Application of dichloromethane vapour to a drop cast sample on a glass slide. (Right) Application of water to the same sample to return it to the orange form.

cause this transition, however water vapour produced by bubbling nitrogen through warmed water causes a rapid transition. This need for a higher humidity to cause the change may indicate that this complex may have a use in humidity sensor applications.

The reversibility of this transition is also different to that observed for **1**. For **3**, some thin film samples, the transition to green became slower/less complete with repeated transitions, and unless re-precipitated the sample eventually became permanently orange. Investigation into why this may be, led to the realisation that the substance has a high affinity for crystallisation with dichloromethane, and it is proposed that this non-vapochromic solvate may result in a more stable structural configuration, resulting in eventual transformation to this form. In response to this, the solid was dissolved in acetone and repeatedly dried rapidly under heat and vacuum to try and remove residual crystallised dichloromethane from the reaction conditions. The solid was then dissolved in hot isopropanol and precipitated as green solid. This solid transitions between green and orange forms which were then fully reversible.

The nature of these transitions was investigated in the same manner as for **1**, with the additional advantage of having a detailed understanding of the process in **1**. It would, for instance, be a reasonable assumption that the rapid switching between coloured forms is again due to a structural rearrangement facilitating varying degrees of inter-metallic overlap. It may also be hypothesised that due to the orange form being produced upon exposure to water, that a form structurally similar to that of the red form of **1** could be produced, with the water hydrogen bonding to the cyanide ligands.

The green form however is not as easily explainable. The compound does not initially appear to uptake any solvent into the structure, given that multiple solvents result in the same visual response, including the non-hydrogen bonding solvent dichloromethane (although residual water may be present). It was therefore proposed that the green form is perhaps analogous to the solvent-free, yellow form of **1**, and the solvent vapour acts to displace the bound water molecules. However, transition to the green form was not producible with heat, vacuum, or dry gas flow. An alternative explanation could be that both forms, orange and green, are water adducts and the difference between them is the number of water molecules absorbed. The orange form could contain more water molecules that prevents stacking between the Pt centres while the green form with fewer water molecules, using only solvent vapour, results in better Pt···Pt overlap in the stacks.

Absorption spectroscopy of the two forms of 3. UV-visible absorption spectroscopy was also performed on the yellow/orange and green forms of **3** in the solid state on thin films. As can be seen in Fig. 13, upon application of solvent vapour, a completely new absorption at 600 nm appears, indicating a new lower energy transition. This suggests that as with **1**, a change in solvent occupation may be inducing a structural change leading to an increase in platinum d_{z^2} interaction.

Powder X-ray diffraction studies of 3. Powder diffraction studies were performed on the yellow and green forms of **3**. However, both forms were amorphous, lacking long range order. Thus, it was not possible to follow the transformations by X-ray powder diffraction.

Single crystal X-ray structure determination of the yellow/orange form of 3. The production of single crystal forms of **3** were attempted, but not surprisingly from the X-ray powder study no crystalline forms with vapochromic properties

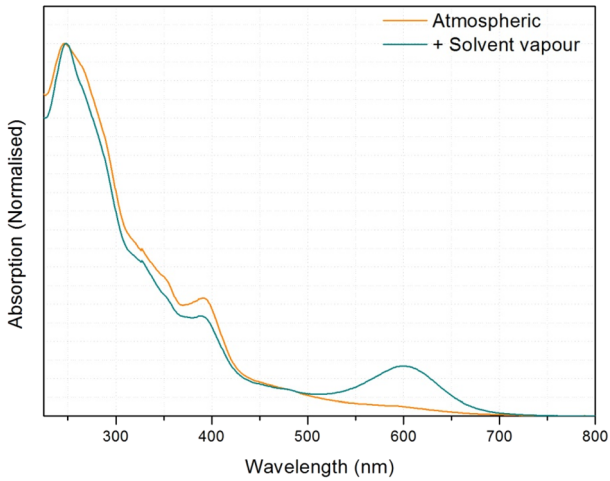

Fig. 13 UV-visible spectrum of **3** before and after solvent vapour application.

could be produced. Only non-solvent-sensitive yellow crystals were obtained, from slow evaporation of dichloromethane solution, and the crystals were found to be a dichloromethane solvate (Fig. 14).

The complex **3** crystallised in the triclinic space group $P\bar{1}$, with two independent neutral molecules of **3**, and one of dichloromethane, in the asymmetric unit

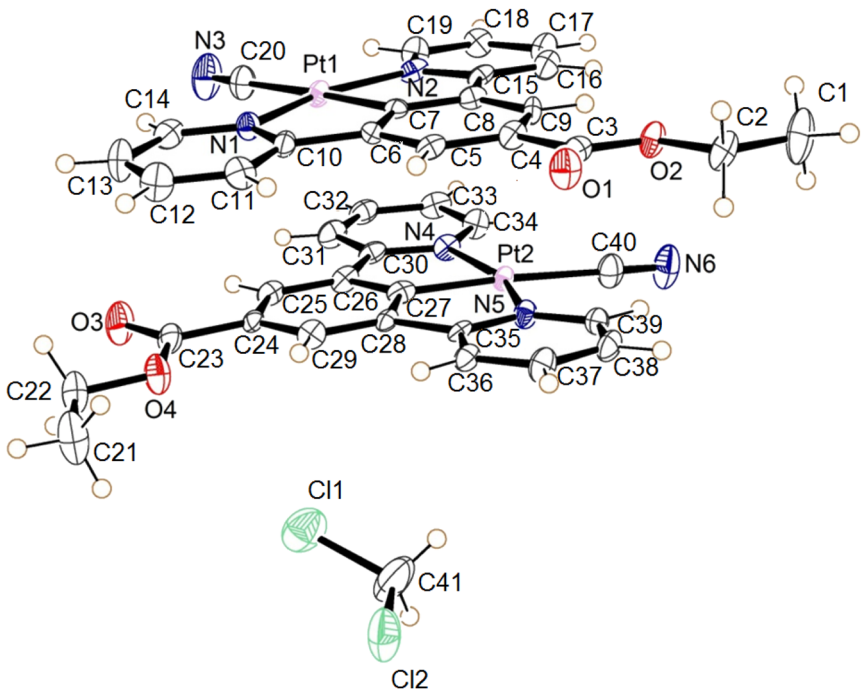

Fig. 14 The molecular structures of the two independent molecules of the dichloromethane solvate of **3**, the displacement ellipsoids are shown with 50% probability.

Table 6 The bond parameters describing the coordination geometry of the two independent Pt(II) centres in the yellow form of **3**

Bond	Length (Å)
Pt1–N1	2.023 (5)
Pt1–N2	2.050 (7)
Pt1–C7	1.943 (6)
Pt1–C20	2.089 (7)
C20–N3	1.120 (10)
Bond	**Length (Å)**
Pt2–N4	2.051 (6)
Pt2–N5	2.054 (6)
Pt2–C27	1.938 (7)
Pt2–C40	2.078 (7)
C40–N6	1.129 (9)

Table 7 The C–H donor hydrogen bonding interactions in the yellow form of **3**

Bond[a]	Distance (D···A) (Å)	Distance (H···A) (Å)	Angle (D···H···A) (°)
C31–H23–Cl2^{1}	3.759 (8)	2.840	170.16
C13–H10–Cl2^{2}	3.469 (9)	2.820	127.87
C12–H9–Cl2^{2}	3.532 (8)	2.939	122.93
C38–H29–N6^{3}	3.546 (10)	2.777	140.80
C21–H17–N3^{4}	3.486 (11)	2.730	136.15
C18–H14–N6^{5}	3.450 (12)	2.590	153.93
C13–H10–O3^{4}	3.2215 (09)	2.471	137.90
C33–H25–N6^{5}	3.557 (10)	2.867	131.84
C32–H24–O1^{6}	3.574 (9)	2.651	172.03

[a] $1 = (x, 1+y, z)$, $2 = (1-x, 1-y, -z)$, $3 = (1-x, 1-y, 1-z)$, $4 = (1-x, 2-y, -z)$, $5 = (1-x, 2-y, 1-z)$, $6 = (1+x, 1+y, z)$.

of the unit cell. The molecular structure of the independent molecules is similar to that of **1**, with the ester groups lying close to the plane of the pincer ligand. The platinum centres adopt the expected square planar geometry with minor distortion (N1–Pt1–N2 angle 160.3° (2) and N4–Pt2–N5 angle 159.7 (2)°) due to the pincer bite angle. Bond parameters are within expected range (Table 6).[39–41] The extended structure has the molecules lying in planes, however Pt···Pt separation between the layers is 4.6139(5) Å suggesting no interaction. Weak C–H donor hydrogen-bonding to the dichloromethane, cyanide and carboxylate groups is also present in the structure. Details of these interactions are listed in Table 7.

Cyano[phenyl 3,5-di(2-pyridyl)benzoato]platinum (4)

Synthesis and characterisation of complex 4. Given that the ethyl ester pincer complex **3** displayed vapochromic properties, but lacked long range order in its solid structure, an inherently more ordered alternative ester analogue was prepared. A phenyl analogue was chosen, as it displays rigidity along with the

possibility of π-stacking interactions, hopefully allowing a more ordered vapochromic structure to form. The pincer ligand ester was synthesised by esterifying 1,3-dibromobenzoic acid, and then the complex **4** was prepared using the same methodology as for complex **3**.

The pincer complex **4** was fully characterised by NMR and IR spectroscopy, and by mass spectrometry. The presence of the phenyl group was clearly indicated by ^{1}H NMR spectroscopy. The IR spectrum shows a strong, sharp absorption at 2116 cm^{-1}, assignable to the $\nu_{C\equiv N}$ of a cyanide group. This value is consistent with those recorded for a series of related compounds.[43,44] Also seen is a single strong absorption at 1725 cm^{-1} assignable to the $\nu_{C=O}$ of the ester group, which is a typical value for a benzoate ester.

Vapochromic and solvatochromic behaviour of complex 4. The complex **4** displays vapochromic behaviour. It can be precipitated from dichloromethane/methanol or dichloromethane/tetrahydrofuran solution as a purple film (Fig. 15(a)), which is extremely sensitive to gentle vapour flow (air squeezed from solvent wash bottle with straw removed) of a variety of polar solvents: methanol, dichloromethane, ethanol, acetone, isopropanol (in order of decreasing sensitivity). Each solvent appears to elicit the same response, whereby the compound transforms to a cherry red colour (Fig. 15(b) and (c)). However, upon direct application of liquid methanol or dichloromethane, the film appears to dry with a greenish colour (Fig. 15(d)). This greenish film is still sensitive to the same solvent conditions and turns to the same cherry red colour over time.

X-ray powder diffraction study of the forms of 4. Powder diffraction experiments were performed to determine whether forms of complex **4** display long range order. A capillary was prepared containing the freshly precipitated powder first, and an experiment run. The same capillary was then filled with a small amount of methanol, turning the powder red, and the experiment repeated. It was determined that unlike **3** the powders were indeed crystalline, although the diffraction data was poor (Fig. S6†), although there were significant differences between the patterns for the purple and red powders.

Attempted single crystal X-ray structure determination of 4. Attempts were made to crystallise **4** by evaporation in a form representative of the vapochromic films but, unfortunately, only microcrystals that were too small for single crystal X-ray diffraction studies to be carried out formed. The microcrystals appear green to the naked eye but were revealed to display dichroism under turning polarising

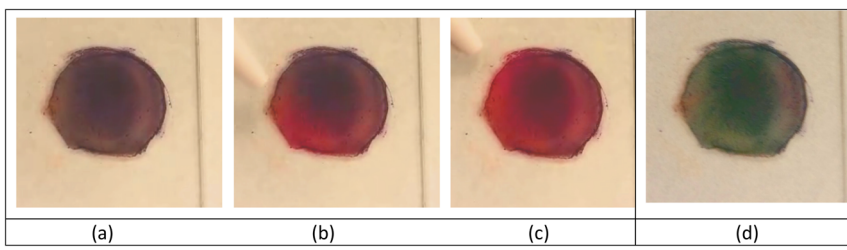

Fig. 15 Observation of the vapochromic properties of a drop-cast-thin film (from methanol/dcm solution) (*ca.* 2 cm in diameter) of **4** and its response to a gentle flow of methanol vapour and after washing with methanol and drying. (a) Purple film on precipitation, (b) turning red upon a gentle flow of solvent vapour, (c) red colouration after solvent vapour treatment, (d) after washing with methanol and drying.

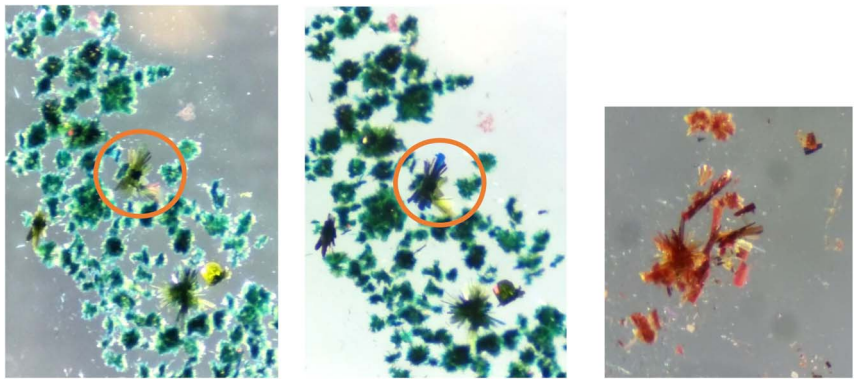

Fig. 16 (Left/middle) Dichroism seen in crystals of **4** under two orientations of polarising filter. Within the circle in both photographs is the same cluster of crystals. (Right) The same crystals after exposure to air.

filters, where the larger crystals could be seen to transform between blue and yellow (Fig. 16). The crystals were extremely air sensitive, changing to red immediately upon direct air exposure, and after a few minutes under Fomblin oil.

Although the structure could not be established it is likely by comparison with the other members of the series and because of its observed vapochromic behaviour is likely that the crystal is porous, and hydrogen bonds will be formed with hydrogen bond donor solvents. By changing the solvent that the crystalline material is exposed to, through exchange of solvents in the cavities within the crystal a variety of crystalline forms will result, exhibiting different metal···metal interactions and different colours.

Conclusions

This study shows that the incorporation of an acyl or ester substituent (R) on the central ring in a (N^C^N) pincer ligand coupled with the coordination of a small, strong field cyanide ligand to the central Pt atom, with the general formula [Pt(N^C(R)^N)(CN)], results in the formation of complexes that undergo thermochromic or vapochromic/solvatochromic behaviour. The presence of the smaller acyl substituent results in a thermochromic solid, as solvent water is lost from the complex (**2**), while with the larger ethyl (**3**) and phenyl (**4**) esters, along with the previously reported methyl ester analogue (**1**)[30] the solids display a range of rapidly reversible vapochromic or solvatochromic behaviour with a range of solvents and show some selectivity.

An analysis of the factors that can be correlated with the behaviour suggests that the cyanide ligand plays an important role, since simple [Pt(N^C^N)Cl] complexes have been extensively studied and their luminescent properties investigated[3,11] but have not been reported to show vapochromic behaviour, to our knowledge, although substituted pincer ligand systems have. The cyanide ligand may have certain advantages over the chloride. In the case of complexes **1–4** the cyanide ligand serves not only as a hydrogen bonding site for solvent uptake, but as a facilitator for the colour changing interactions by allowing the stabilisation of

the HOMOs with which it shares π-interactions, allowing for a prominent non-bonding d_{z^2} orbital relative to the frontier orbitals.

The size and hydrogen bonding capabilities of the substituents on the central ring of the pincer ligand also play a significant role in determining the vapochromic properties. For example, in our hands, the simple [Pt(N^C^N)(CN)] complex, with no substituent on the central ring, does not show vapochromic responses to common volatile organic solvents.[45] The bulkier the substituent the less efficiently do the pincer molecules pack in the solid state, thus creating a greater void space for the solvents or vapours to diffuse through the crystal. Similar effects have been seen for pincer complexes with substituents on the two pyridyl rings of the N^C^N pincer ligand.[21,22] Additionally, the acetyl and ester groups form hydrogen bonded networks running through the crystals, generating channels through which the solvents and vapours can pass, allowing the rapid dynamic colour changes to occur.

In some cases, the pincer complexes show particular selectivity towards particular solvents and vapours. For complex **1** the solid is red in the presence of water and blue in the presence of methanol,[30] while for complexes **3** and **4**, the colour change is less dependent on the specific solvent used. For example, **3** shows the same colour change for methanol, ethanol or dichloromethane (although residual water may be present in the solvents), and for **4** the colour changes are even more complex. This selectivity can be related to the hydrogen bonding in the material and the influence that this has on the stacking of the layers and the intermetallic d_{z^2}–d_{z^2} interactions between the adjacent Pt centres, which is at least partially responsible for the colour of the complexes.

While this study does not rationalise the vapochromic behaviour of platinum pincer complexes fully, it does highlight some of the factors that favour rapidly reversible vapochromic behaviour, and benchmark some of the crystal engineering protocols that would be useful for the design of such materials. There would be many industrial applications of such a protocol with platinum vapochromic compounds as practical chemosensor devices being considered a promising prospect.[46] Several attempts have been made at immobilising a vapochromic material into a polymer substrate in order to create "smart coatings" for chemical sensing applications.[31,47]

Author contributions

M. J. B. and S. F. are responsible for the synthesis reported in the paper, and M. J. B. performed the spectroscopic and vapochromic and solvatochromic studies. M. J. B., L. E. H. and L. H. T. undertook the structural studies and interpretation of the data. M. J. B. and L. H. T. are responsible for the first draft of the paper. P. R. R. is responsible for the conceptualisation of the project, for reviewing and editing the manuscript, and for project administration and funding acquisition.

Conflicts of interest

There are no conflicts to declare.

Acknowledgements

We are grateful to the Engineering and Physical Sciences Research Council (EPSRC) for a Programme Grant (grant no. EP/K004956/1). The project was also

supported by EPSRC grant EP/101974X. SF is grateful for the support of a fellowship from the European Commission, under the Marie Curie Intra European Fellowship Scheme (PIEF-GA-2009-252883; SFL-PRR).

References

1 Q. Zhao, F. Li and C. Huang, *Chem. Soc. Rev.*, 2010, **39**, 3007–3030.
2 M. Kato, *Bull. Chem. Soc. Jpn.*, 2007, **80**, 287–294.
3 L. J. Grove, J. M. Rennekamp, H. Jude and W. B. Connick, *J. Am. Chem. Soc.*, 2004, **126**, 1594–1595.
4 L. J. Grove, A. G. Oliver, J. A. Krause and W. B. Connick, *Inorg. Chem.*, 2008, **47**, 1408–1410.
5 J. Fornies, S. Fuertes, J. A. Lopez, A. Martin and V. Sicilia, *Inorg. Chem.*, 2008, **47**, 7166–7176.
6 Y. Shigeta, A. Kobayashi, T. Ohba, M. Yoshida, T. Matsumoto, H. C. Chang and M. Kato, *Chem.–Eur. J.*, 2016, **22**, 2682–2690.
7 S. D. Taylor, W. Howard, N. Kaval, R. Hart, J. A. Krause and W. B. Connick, *Chem. Commun.*, 2010, **46**, 1070–1072.
8 S. Chatterjee, A. E. Norton, M. K. Edwards, J. M. Peterson, S. D. Taylor, S. A. Bryan, A. Andersen, N. Govind, T. E. Albrecht-Schmitt, W. B. Connick and T. G. Levitskaia, *Inorg. Chem.*, 2015, **54**, 9914–9923.
9 V. M. Shingade, L. J. Grove and W. B. Connick, *Dalton Trans.*, 2020, **49**, 9651–9661.
10 M. L. Muro, C. A. Daws and F. N. Castellano, *Chem. Commun.*, 2008, 6134–6136.
11 V. W. W. Yam, K. H. Y. Chan, K. M. C. Wong and N. Y. Zhu, *Chem.–Eur. J.*, 2005, **11**, 4535–4543.
12 P. W. Du, J. Schneider, P. Jarosz, J. Zhang, W. W. Brennessel and R. Eisenberg, *J. Phys. Chem. B*, 2007, **111**, 6887–6894.
13 T. J. Wadas, Q. M. Wang, Y. J. Kim, C. Flaschenreim, T. N. Blanton and R. Eisenberg, *J. Am. Chem. Soc.*, 2004, **126**, 16841–16849.
14 D. J. Cardenas, A. M. Echavarren and M. C. R. de Arellano, *Organometallics*, 1999, **18**, 3337–3341.
15 J. A. G. Williams, A. Beeby, E. S. Davies, J. A. Weinstein and C. Wilson, *Inorg. Chem.*, 2003, **42**, 8609–8611.
16 J. A. G. Williams, *Chem. Soc. Rev.*, 2009, **38**, 1783–1801.
17 S. Fuertes, S. K. Brayshaw, P. R. Raithby, S. Schiffers and M. R. Warren, *Organometallics*, 2012, **31**, 105–119.
18 S. Fuertes, C. H. Woodall, P. R. Raithby and V. Sicilia, *Organometallics*, 2012, **31**, 4228–4240.
19 Y. Nishiuchi, A. Takayama, T. Suzuki and K. Shinozaki, *Eur. J. Inorg. Chem.*, 2011, 1815–1823.
20 C. Y. Lien, Y. F. Hsu, Y. H. Liu, S. M. Peng, T. Shinmyozu and J. S. Yang, *Inorg. Chem.*, 2020, **59**, 11584–11594.
21 P. Pander, A. Sil, R. J. Salthouse, C. W. Harris, M. T. Walden, D. S. Yufit, J. A. G. Williams and F. B. Dias, *J. Mater. Chem. C*, 2022, **10**, 15084–15095.
22 S. Hattori, T. Nakano, N. Kobayashi, Y. Konno, E. Nishibori, T. Galica and K. Shinozaki, *Dalton Trans.*, 2022, **51**, 15830–15841.
23 S. J. Farley, D. L. Rochester, A. L. Thompson, J. A. K. Howard and J. A. G. Williams, *Inorg. Chem.*, 2005, **44**, 9690–9703.

24 J. A. G. Williams, S. Develay, D. L. Rochester and L. Murphy, *Coord. Chem. Rev.*, 2008, **252**, 2596–2611.
25 W. A. Tarran, G. R. Freeman, L. Murphy, A. M. Benham, R. Kataky and J. A. G. Williams, *Inorg. Chem.*, 2014, **53**, 5738–5749.
26 A. Kobayashi, T. Yonemura and M. Kato, *Eur. J. Inorg. Chem.*, 2010, 2465–2470.
27 Y. Kunugi, K. R. Mann, L. L. Miller and C. L. Exstrom, *J. Am. Chem. Soc.*, 1998, **120**, 589–590.
28 K. M. C. Wong and V. W. W. Yam, *Acc. Chem. Res.*, 2011, **44**, 424–434.
29 S. C. F. Kui, S. S. Y. Chui, C. M. Che and N. Y. Zhu, *J. Am. Chem. Soc.*, 2006, **128**, 8297–8309.
30 M. J. Bryant, J. M. Skelton, L. E. Hatcher, C. Stubbs, E. Madrid, A. R. Pallipurath, L. H. Thomas, C. H. Woodall, J. Christensen, S. Fuertes, T. P. Robinson, C. M. Beavers, S. J. Teat, M. R. Warren, F. Pradaux-Caggiano, A. Walsh, F. Marken, D. R. Carbery, S. C. Parker, N. B. McKeown, R. Malpass-Evans, M. Carta and P. R. Raithby, *Nat. Commun.*, 2017, **8**, 1800.
31 C. M. Sangan, O. J. Pountney, J. A. Scobie, B. Cochrane, C. Stubbs and P. R. Raithby, *Int. J. Heat Mass Transfer*, 2018, **127**, 437–446.
32 M. C. Burla, R. Caliandro, M. Camalli, B. Carrozzini, G. L. Cascarano, L. De Caro, C. Giacovazzo, G. Polidori, D. Siliqi and R. Spagna, *J. Appl. Crystallogr.*, 2007, **40**, 609–613.
33 G. M. Sheldrick, *Acta Crystallogr., Sect. C: Struct. Chem.*, 2015, **71**, 3–8.
34 O. V. Dolomanov, L. J. Bourhis, R. J. Gildea, J. A. K. Howard and H. Puschmann, *J. Appl. Crystallogr.*, 2009, **42**, 339–341.
35 G. Nolze and W. Kraus, *Powdercell 2.3*, Federal Institute for Materials Research and Testing, Berlin, 2000.
36 W. Lu, B.-X. Mi, M. C. W. Chan, Z. Hui, C.-M. Che, N. Zhu and S.-T. Lee, *J. Am. Chem. Soc.*, 2004, **126**, 4958–4971.
37 S. J. Choi, J. Kuwabara, Y. Nishimura, T. Arai and T. Kanbara, *Chem. Lett.*, 2012, **41**, 65–67.
38 K. Mizuse, *Spectroscopic Investigations of Hydrogen Bond Network Structures in Water Clusters*, Springer Science & Business Media, 2013.
39 M. S. Khan, M. K. Al-Suti, M. R. A. Al-Mandhary, B. Ahrens, J. K. Bjernemose, M. F. Mahon, L. Male, P. R. Raithby, R. H. Friend, A. Kohler and J. S. Wilson, *Dalton Trans.*, 2002, 65–73.
40 J. R. Berenguer, E. Lalinde and J. Torroba, *Inorg. Chem.*, 2007, **46**, 9919–9930.
41 Y. Chen, K. Li, W. Lu, S. S.-Y. Chui, C.-W. Ma and C.-M. Che, *Angew. Chem., Int. Ed.*, 2009, **48**, 9909–9913.
42 J. K. Stille, *Angew. Chem., Int. Ed. Engl.*, 1986, **25**, 508–524.
43 A. A. Lemus-Santana, J. Rodríguez-Hernández, L. F. delCastillo, M. Basterrechea and E. Reguera, *J. Solid State Chem.*, 2009, **182**, 757–766.
44 T. Kayano, S. Takayasu, K. Sato and K. Shinozaki, *Chem.–Eur. J.*, 2014, **20**, 16583–16589.
45 M. J. Bryant, Platinum Pincer Complexes: in Pursuit of Switchable Materials, PhD Thesis, University of Bath, 2015.
46 A. Kobayashi and M. Kato, *Eur. J. Inorg. Chem.*, 2014, **2014**, 4469–4483.
47 J. R. Kumpfer, S. D. Taylor, W. B. Connick and S. J. Rowan, *J. Mater. Chem.*, 2012, **22**, 14196–14204.